



Flood risk assessment of a small river with limited available data

Noémi Mária Szopos¹ · Imre J. Holb^{2,3} · Abriha Dávid¹ · Szilárd Szabó¹

Received: 1 May 2024 / Revised: 18 August 2024 / Accepted: 19 August 2024
© The Author(s) 2024

Abstract

Flood risk modeling of small watercourses is challenging when only limited input data are available. Therefore, this study assessed the flood characteristics of a small river (Tarna River: entire watershed-C, upper-VS, middle-TMS, and lower section-TOS) from 1990 to 2019. The assessment focused on modeling, model calibration, and validation using feature event-based time-series data in data-scarce environments. We showed that since the 2000s, the number of high-water levels above 250 cm, and the frequency of three flood types had increased. Flood simulation results showed the largest flooded area in the TMS section, followed by the VS, and then the TOS. The outcomes from the VS, TMS, and TOS sections did not exhibit superior performance compared to the C area. Models performed well for larger flood events, with Kling Gupta Efficiency corresponding well to NRMSE and Nash-Sutcliffe efficiency metrics. Accordingly, flood events characterized by the longest duration and high-water levels yielded outstanding results across all areas, followed by moderate flood events with good accuracy. Normal water level events exhibited significant deviations from the reference across all sections. In summary, despite the event-based modeling challenges in data-limited environments, such models can still mitigate potential flood events and improve decision-making processes.

Keywords Hydrological modeling · HEC-RAS · Model accuracy · Flood events

1 Introduction

The impacts of climate change are becoming increasingly perceptible owing to shifting average temperature values, the emergence of anomalies, and the growing frequency of extreme weather events. Consequently, natural disasters, societal changes, and economic shifts occurred. Studies indicate that Earth's surface temperature exhibits an increasing trend [1]. Previous research has also confirmed that due to decreasing summer precipitation and increasing spring evaporation, the values of temperature anomalies and

the frequency of summer droughts in Central Europe and the Carpathian Basin show an increasing trend [2–4].

The global frequency of natural disasters, particularly the occurrence of severe floods, has increased [5, 6]. Large-scale inundations from river flooding have caused extensive damage and have had a global impact on economic activities, built environments, infrastructure, ecosystems, agriculture, and the natural environment [5]. However, major river floods pose a threat and even smaller, rapidly occurring river floods can lead to considerable damage. This phenomenon has also been observed in Hungary [7, 8].

Early intervention, predictive systems, and hydrological models can significantly assist in the event of sudden floods. The current conventional tools present challenges in terms of timely forecasting, making it necessary to introduce new methods. Flood preparedness and innovative flood management can help mitigate damage [6]. The use of numerical models has gained prominence in research [9, 10]. In hydrological studies, modeling offers the opportunity for both permanent and non-permanent runs, enabling the examination of temporal and spatial variations in events and modeling of various flood discharges [11]. However, it is crucial to understand the applications and objectives of these models.

✉ Imre J. Holb
holbimre@gmail.com; holb@agr.unideb.hu

¹ Department of Physical Geography and Geoinformatics, Faculty of Sciences and Technology, University of Debrecen, Egyetem tér 1, Debrecen 4032, Hungary

² Institute of Horticulture, Faculty of Agricultural and Food Sciences and Environmental Management, University of Debrecen, Böszörményi Str. 138, Debrecen 4032, Hungary

³ Centre for Agricultural Research, Plant Protection Institute, Hungarian Research Network (HUN-REN), Herman Ottó út 15, Budapest, Budapest 1022, Hungary

Hydrodynamic models allow the tracking of flow, determination of water depths, simulation of flood wave propagation, and simulation of precipitation runoff at the watershed scale. The location and extent of the potential inundation areas can be defined. A comprehensive understanding of a flood event can only be achieved by analyzing and drawing conclusions after merging the information [11, 12].

For small watercourses, several factors complicate the construction of models, determination of their accuracy, and assessment of the relevance of the results. The first and most important factor is the resolution and accuracy of the available basic data because it is necessary to use a more detailed DTM base for a reconstructed flood wave during the recession of a small watercourse [13, 14]. When modeling small watercourses, it is essential to define the banks as accurately as possible and mark terrain features to determine sensitive bank sections and load levels as accurately as possible. Determining the load levels is a vital part of operational forecasting. One illustrative example is the spring flood on the Tisza River in 2000, where Highway 41 had to be cut during the flood because this road section functioned as a dam element. The bridges and culverts were unable to drain a large amount of water, resulting in flooding of seven settlements. The defenses had to face a flood of unprecedented magnitude on the Tisza River, and flood waves also formed on the tributaries due to the effects of the backwater, while the dyke breached in 2001 further supported the further development of localization plans [7, 15]. Another complicating factor is the absence of gauging stations during a receding flood wave, resulting in significant information gaps. As emphasized by Sziebert and Zellei [16], flood flow measurements aim to facilitate understanding through measurement series and analysis, which we deemed necessary in this study.

Current studies suggest utilizing international databases and new remote sensing techniques when creating models and hydrological studies that ensure data reliability and uniformity, and consequently, the widespread acceptance and relevance of the results [17, 18]. Studies have been conducted on the possibility of applying hydrological modeling at both national and international levels. However, there is still room for refining this information and expanding our experience [12, 19–22]. HEC-RAS (USACE-CEIWR-HEC) is a freely accessible, internationally recognized, and widely used program for modeling hydrological processes. The model is applicable to both complex studies and small watercourses and is compatible with other geoinformation software. Previous research has demonstrated that HEC-RAS is particularly suitable for river channel modeling, cross-sectional representation, and combined analysis of multiple parameters and is capable of simulating surface profiles during various flood events [11, 23, 24]. Field

measurements and digital modeling can be effectively combined for surface water flow modeling [20], and integrating HEC-RAS with other models has proven to be suitable for improving the accuracy of traditional forecasts and serves as a valuable tool for flood risk management [25]. However, the results of studies on data-scarce and large-scale watercourses require further investigation [22, 23]. Flood modeling has already been conducted for Hungary's large rivers, and in recent decades, the models have been improved with an increasing focus on detailed surveying and mapping. Special and important roles are given to understanding the formation and changes of flood waves in the Tisza and Danube Rivers [26, 27]. Kovács et al. [28] and colleagues demonstrated the significance of floods using the example of the Tisza River. Nagy [29] stated that floodplains are one of the most important elements in the runoff of flood events, and that surveying and modeling these areas is an urgent task to ensure long-term flood safety. Gashi et al. [30] investigated the lower reaches of the Drava River, emphasizing how the runoff from flood events influenced channel evolution. However, smaller streams remain in the background and in many cases, understanding of flood situations is incomplete and the Tarna river is a representative example. The data-poor environment includes lack of high-resolution topographic data, few water gauge stations, few official cross-sections, accurate delineation of the riverbank, a database of tributary flow rates, and the extent of vegetation along the river.

We aimed to provide a flood inundation model for the most relevant flood events that occurred within the watershed of the Tarna River (Hungary) using a comprehensive approach that utilized integrated data sources, including satellite imagery, water gauge data, and land-use information. Although various attempts have been made to model larger rivers, modeling flood situations in smaller rivers with limited observed data remains a challenge, while the risk of sudden, large-scale floods in lowland and hilly regions in Hungary is high [9]. From this perspective, the Tarna Watershed is of particular importance. Although the watercourse is a relatively small river, floods and flash floods have already caused damage in this area. Flood surges rapidly inundate an area and their duration typically spans a few days. In extreme cases, the descending water volume can reach up to 50–70 million m³. Although flood modeling (especially HEC-RAS) is not a new topic, examining and integrating data-scarce segments is still a research field in which substantial knowledge is missing. The lack of observed data remains an issue for catchments of smaller rivers and poses a significant risk for inappropriate projection possibilities to plan prevention.

This research represents an innovative advancement at a region-specific level as our findings demonstrate that HEC-RAS models are suitable for modeling small streams even

with varying terrain conditions. The research process can serve as a potential scenario for modeling and predicting flood disasters in similarly data-poor environments with similarly diverse terrain conditions. Accordingly, our main objective was to provide flood risk assessment of a small river by assessing the possibilities of modeling, model calibration, and validation considering topographic features based on event-based time-series data in data-scarce environments. Accordingly, our main objective was to provide flood risk assessment of a small river by assessing the possibilities of modeling, model calibration, and validation considering topographic features based on event-based time-series data in data-scarce environments. We had the following hypotheses: (i) number of flood events had increased in the recent decades, and (ii) the river section as well as (iii) the water level (i.e. flood intensity) have relevant effect on the accuracy of the models.

2 Materials and methods

2.1 Study area

The study area, which encompasses the watershed of the Tarna River, is located near the northern Slovakian border of Hungary. It includes streams and tributaries running through the eastern part of the Mátra Mountains and the western side of the Bükk Mountains (Fig. 1). The Tarna catchment area is part of the Tisza River system, covering an area of 2116 km².

The upper section of the Tarna River features hilly terrain, transitioning into a lowland character as it flows towards its mouth. The northern part of the catchment area is primarily characterized by clayey forest soil, but it also contains significant portions of loose limestone-based soils, contributing a substantial part of the Tarna sediment yield [31]. Chernozem-brown forest soil and brown earth can be found in foothill areas. In the southern region, the chernozem soils contain calcareous sediments.

The lowest point of the catchment was 91 m a.s.l., while the highest one was 1014 m (Kékestető), with an average elevation of 219 m across the area. The terrain of the catchment area is diverse, featuring mountainous parts and valleys of streams, and hills and plains of foreland. Generally, the northern part has a larger relief with steeper slopes, and the southern part is rather lowland [31]. Accordingly, the flood characteristics are also different, with quick floods in the north and longer elongated flood curves in the south. The annual mean temperature is 9.5–10.5 °C, but higher regions are colder (7 °C). The annual mean precipitation is 500–550 mm in the lowest areas but can reach 750–800 mm in the Mátra region, peaking in June. Over the past 25 years,

significant daily precipitation data have been recorded at various stations, such as 140.6 mm at Kékestető, 135 mm in Verpelét, and 128.6 mm in Tarnaméra.

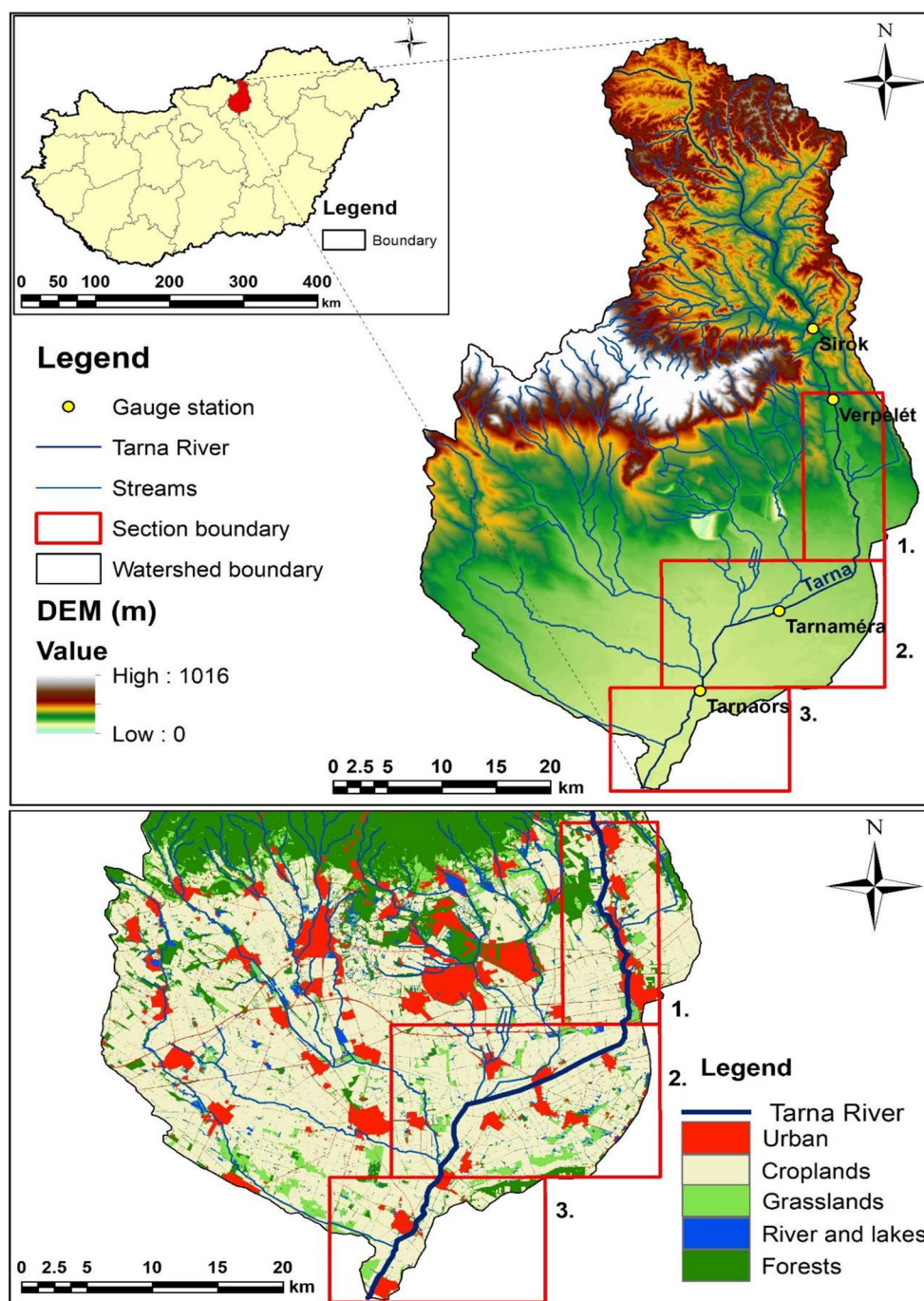
For a detailed analysis, we delineated three distinct sections along the river based on the characteristics of the river: the upper section (VS), middle section (TMS), and lower section (TOS) (Fig. 1). In VS, the elevation values ranged from 107 to 236 m, with a general downhill gradient from north to south. The area is characterized by narrow valleys and steeper slopes (up to 46°). Densely populated areas and villages are located near rivers, posing threats to human lives and property. The TMS also exhibited a decrease in elevation from north to south, with elevation values ranging from 92 to 120 m. Although the slope is rather gentle, the steepness can reach 40°. The land use is predominantly agricultural; however, residential areas can also be found. The TOS features a river section with a wider channel and higher embankment for protection. The elevation mainly ranges from 90 m to 110 m with predominantly gentle slopes. Land use includes agricultural areas and grasslands with several settlements.

Streams originating from the Mátra Mountains can significantly influence Tarna's discharge. The Tarnóca, Bene, and Gyöngyös streams can transport 30–40 m³/s each. These streams flow into Tarna between Tarnaméra and Tarnaörs, contributing to discharge levels of up to 70–80 m³/s for Tarnaméra and 180 m³/s for Tarnaörs.

2.2 Datasets

The analysis required detailed resolution of the spatial data to build the river hydrodynamic model. We utilized two digital elevation models (DEMs) to extract topographic features: (i) the DDM5, developed by the Lechner Knowledge Center (Hungary), from contours 5 × 5 m using interpolation and updated with stereophotogrammetric evaluation, and (ii) the SRTM v4 (Shuttle Radar Topography Mission). Furthermore, the model requires soil and land-use data. Accordingly, we utilized the Corine Land Cover, AGROTOPO (1:100,000 scale), and the Hungary Ecosystem Basemap NÖSZTÉP [32]. Additional topographical and hydrological datasets, including water level and discharge data for the model construction, were provided by ÉMVIZIG. The preparation of topographical data, determination of the terrain's topographical characteristics, delineation of the areal units, and creation of resulting maps were carried out in the QGIS 3.6 software environment [33]. Hydrological models for various events, as well as extracting data for inundation maps and flood events were performed in the HEC-RAS 5.0.7 software environment [34].

Fig. 1 Location of the study area: the watershed of the Tarna River in northern Hungary. Three distinct sections along the river were investigated: the upper section (VS), the middle section (TMS), and the lower section (TOS)



2.3 Data processing and modeling

We compared the flood events of the period of 1990–2004 and 2005–2019 based on the number of flood events, length of floods, and the average number flooding days. Criteria of a flood was the water level > 250 cm, as the water directorate characterizes the flood risks.

Model building is a multistep process, with an initial step involving the selection of events, timing, and discharge values. We analyzed data spanning from 1990 to 2019, and

based on these data, flood events during the period from 2010 to 2019 were significant. Due to the variable flow of the Tarna River, water levels in Verpelét can fluctuate between 11 and 568 cm, with an average discharge of $19.3 \text{ m}^3/\text{s}$ observed at a water level of 300 cm. In Tarnaméra, water levels have ranged from 16 to 500 cm in recent years, with an anticipated average discharge of $10 \text{ m}^3/\text{s}$ at a 300 cm water level. Similarly, water levels in Tarnaörs have historically varied from 65 to 564 cm, correlating to an average discharge of $17 \text{ m}^3/\text{s}$ at a 300 cm water level. These values

are influenced by various topographic and meteorological parameters. Each rainfall event is unique, yet similar values can be forecasted based on multi-year data. The selection of benchmarks was aligned with the official national flood protection levels. During the 2010–2019 period, the two largest floods (LF) of the Tarna River were chosen, where the water level reached or exceeded 350 cm. Two significant flood events (F) were selected in the second category, in which the lowest water level was 200 cm. Next, two average flow events (A) were selected. The time interval for the average water level data was set at 10 day for optimal runtime results and proper consideration of changes in water flow within the area. This category does not include outliers or high-water levels (Table 1).

The catchment geometry of the watershed and sub-watersheds was delineated using the SRTM using the Triangular Irregular Network (TIN) method. This method facilitates precise definition of boundary conditions, sub-basin delineation, and elevation attributes. Topographical data were processed in HEC-RAS 5.0.7, creating a geometric grid for the watershed with a 50 × 50 cell size. However, along rivers and streams, we increased the spatial resolution using DDM5 to better represent the water level variations in the calculations. The roughness coefficient was determined based on the NÖSZTÉP. The geometric grid was completed for the entire watershed (C) as well as the delineated areas of the upper section (VS), middle section (TMS), and lower section (TOS).

The outputs of the simulations contained unsteady flow data for each event at 1-hour intervals. One of the most crucial parameters that has a significant impact on the model simulations is the computation interval. The computation interval should be appropriately small to accurately capture and detect changes in water levels. To calculate the proper time step, it is essential to consider the distance between the cross sections and the flow velocity [34].

Considering the best numerical solution and optimal runtime for model simulations, we applied the following settings, which allowed the models to adequately consider changes. The computation interval was set to 1 min, the mapping output interval was 1 h (h), the hydrograph output interval was 1 h, and the detailed output interval was 1 h. The tolerance intervals were 0.003 m for the water surface and 0.03 m³/s for minimum flow tolerance. Based on the

description of the model runs and our experience so far, these intervals were found to be the most appropriate [34].

Water levels measured at the water gauges were used for validation. During the investigation, we used data from the official gauge stations of Verpelét, Tarnaméra, and Tarnaörs, progressing from north to south. We did not consider the Sirok gauge station because of its very low water levels. We aimed to mitigate uncertainties related to model parameters and input data by observing past events and considering the averaged data.

2.4 Model validation

During the model runs and the subsequent evaluation of results, we had to consider the stability and sensitivity of the model, as well as the factors influencing numerical accuracy. The input data and specified parameters significantly affect the model's sensitivity. The accuracy of geometric data, the precision of boundary conditions, the flow rate and hydrodynamic data, as well as the solution of unsteady flow equations, are crucial during the runs.

We monitored the model's stability primarily after initiating the runs and throughout the process, focusing on the number of iterations and the extent of numerical errors. If the model detected a significant error, the calculation would stop, preventing further runs. In our case, model stability was influenced by parameters such as the geometric mesh, cross sectional geometry, computational time steps, low flow conditions, and missing or inaccurate channel data due to terrain issues. We identified these errors through multiple test runs, collected the data displayed in the computation window, and subsequently corrected them.

If the models did not exhibit instability or errors during the runs, we conducted further accuracy assessments on the results. We inserted multiple cross sections into the model, ensuring they were placed at representative and measurable locations to also verify the boundary conditions. The distance between the cross sections is crucial, as improper spacing can lead to numerical errors or result instability. Profile lines are suitable for calculating the flow rate through the cross sections.

We compared the cross sections generated in the model with officially measured ones, and if the margin of error was considered minimal, the model was deemed acceptable.

Table 1 The data of the examined events at the Verpelét water gauge

Event type	Event	Start Date	Start Time	End Date	End Time	Duration
Largest Flood (LF)	a	20-02-2010	13:00	03-03-2010	23:00	12 days
	b	10-02-2016	14:00	26-02-2016	11:00	17 days
Flood (F) - >200 cm	c	30-03-2013	04:00	09-04-2013	08:00	11 days
	d	04-05-2017	16:00	17-05-2017	07:00	14 days
Average (A)	e	10-02-2011	00:00	19-02-2011	23:00	10 days
	f	06-05-2015	00:00	15-05-2015	23:00	10 days

During the model runs, the Manning's value was considered a fundamental input parameter, and we did not conduct further testing related to changes in it. Water level data from hydrological events were derived from the discharge data used in the HEC-RAS software modeling, and water level data from official hydraulic gauge stations were used. We compared the observed and modelled water levels in the watershed at different spatial scales for three flood types: large floods, floods, and average floods.

The models were evaluated with several accuracy metrics based on the difference between the observed and modelled values (i.e., residuals): correlation, standard deviation, root mean square error (RMSE), normalized root mean square error (NRMSE), unbiased root mean square error (ubRMSE), Kling-Gupta Efficiency (KGE), and Nash-Sutcliffe Efficiency (NSE).

The RMSE measures the average magnitude of the differences between the modelled and observed values, and lower RMSEs indicate better model performance, with smaller average residuals (Eq. 1). The NRMSE is the normalized version of the RMSE indicating the relative magnitude of residuals, where a smaller value indicates better model performance. The ubRMSE measures the square root of the mean squared difference (RMSE), considering the bias.

$$\text{RMSE} = \sqrt{\frac{\sum_{i=1}^N (M_i - O_i)^2}{N}} \quad (1)$$

$$\text{NRMSE} = \sqrt{\frac{\sum_{i=1}^N (M_i - O_i)^2}{\text{nval}}} \quad (2)$$

$$\text{nval} = \left\{ \begin{array}{l} \text{sd}(O), \text{norm} = \text{sd} \\ o_{\max} - o_{\min}, \text{norm} = \text{maxmin} \end{array} \right\} \quad (3)$$

$$\text{bias} = \frac{\sum_{i=1}^N (M_i - O_i)}{\sum_{i=1}^N O_i} \quad (4)$$

$$\text{ubRMSE} = \sqrt{\text{RMSE}^2 - \text{bias}^2} \quad (5)$$

Where,

Table 2 Flood characteristics between the periods of 1990–2004 and 2004–2019 at Tarnaörs, Tarnaméra and Verpelét, Hungary

Floods	Period	Tarnaörs	Tarnaméra	Verpelét
Number of flood events	1990–2004	23	31	6
	2004–2019	53	46	12
Number of days	1990–2004	126	130	15
	2004–2019	355	125	19
Average number of days of flooding	1990–2004	5.48	4.19	2.50
	2004–2019	6.70	2.72	1.58

' M_i ' is the i^{th} element of the modelled data,
' O_i ' is the i^{th} element of the observed data,
' N ' is the number of data points,
' sd ' is the standard deviation, and,
' $maxmin$ ' is the difference between the maximum and minimum values.

NSE is a normalized measure of model performance, which is determined by dividing the summed residual squares by the sum of squares of the observed values and their mean (Eq. 4). Values between 0.75 and 1 indicate very good, 0.65–0.75 good, 0.50–0.65 satisfactory, and < 0.50 unsatisfactory model [35].

$$\text{NSE} = 1 - \frac{\sum_{i=1}^N (M_i - O_i)^2}{\sum_{i=1}^N (O_i - \bar{O})^2} \quad (6)$$

Additionally, we assessed the efficiency of the hydrological models using the KGE, which calculates the correlation and normalized deviations between the predicted and measured data. A value closer to 1 indicates better model performance; generally, values between 0.8 and 1 are excellent, 0.6–0.8 good, 0.4–0.6 satisfactory, and < 0.4 unsatisfactory models.

The obtained results were also summarized in Taylor diagrams illustrating the level of correlation between the observed and modelled values of the water level; a high correlation indicated a greater degree of agreement. The standard deviation (SD) was also visualized to indicate the residuals' SDs, and the RMSE represented the average prediction error. The Taylor diagram provided an overview of the models' performance, and we compared the average progression of events for the entire study area (C), upper section (VS), middle section (TMS), and lower section (TOS).

Statistical evaluations were conducted using the R 3.5.2 software environment [36]. The spatial delineations represented in the diagrams include the entire study area (C), the upper section (VS), the middle section (TMS), and the lower section (TOS) (Fig. 1).

3 Results

3.1 Flood records in the catchment

The flood events of Tarna between 1990 and 2019 had changed. Between 1990 and 2004, the number of floods were lower, usually only the half of the period of 2005–2019 (Table 2). Accordingly, the number of days when the water level was > 250 cm, also changed at all stations, but the largest difference were observed at Tarnaörs. However, the larger number of flood events not necessarily increased

the average length of the floods, it was true only in case of Tarnaörs.

3.2 Flood models

For flood simulations over section C, event L_b exhibited the largest extent, followed by events L_a, F_c, F_d, A_e, and A_f, which showed considerably smaller values. Regarding the spatial distribution during the modeling of the VS, TMS, and TOS sections, the TMS section was the largest area affected by flooding, followed by VS with a smaller inundated area, and then the TOS had only a small flooded area (Fig. 2; Table 3).

3.3 Model assessment

For the entire section (C), similar trends were observed for both the modeled and observed water levels. The water level of A_e was constant, without any corresponding deviations. For A_f, the observed values were always higher than the model values. For F_c, the water levels differed at the peaks with underestimated modeled water levels. F_d model exhibited minimal differences from measured values. In the case of the L_a event, the increase in water levels began earlier in the observed data than in the model data. In the case of L_b, a slight increase in favor of the observed values at the peaks was observed. Across Area C, no significant deviation was observed for the three flood events.

Regarding the TOS section, for events A_e and A_f, only the initial point showed a distinct difference, whereas the

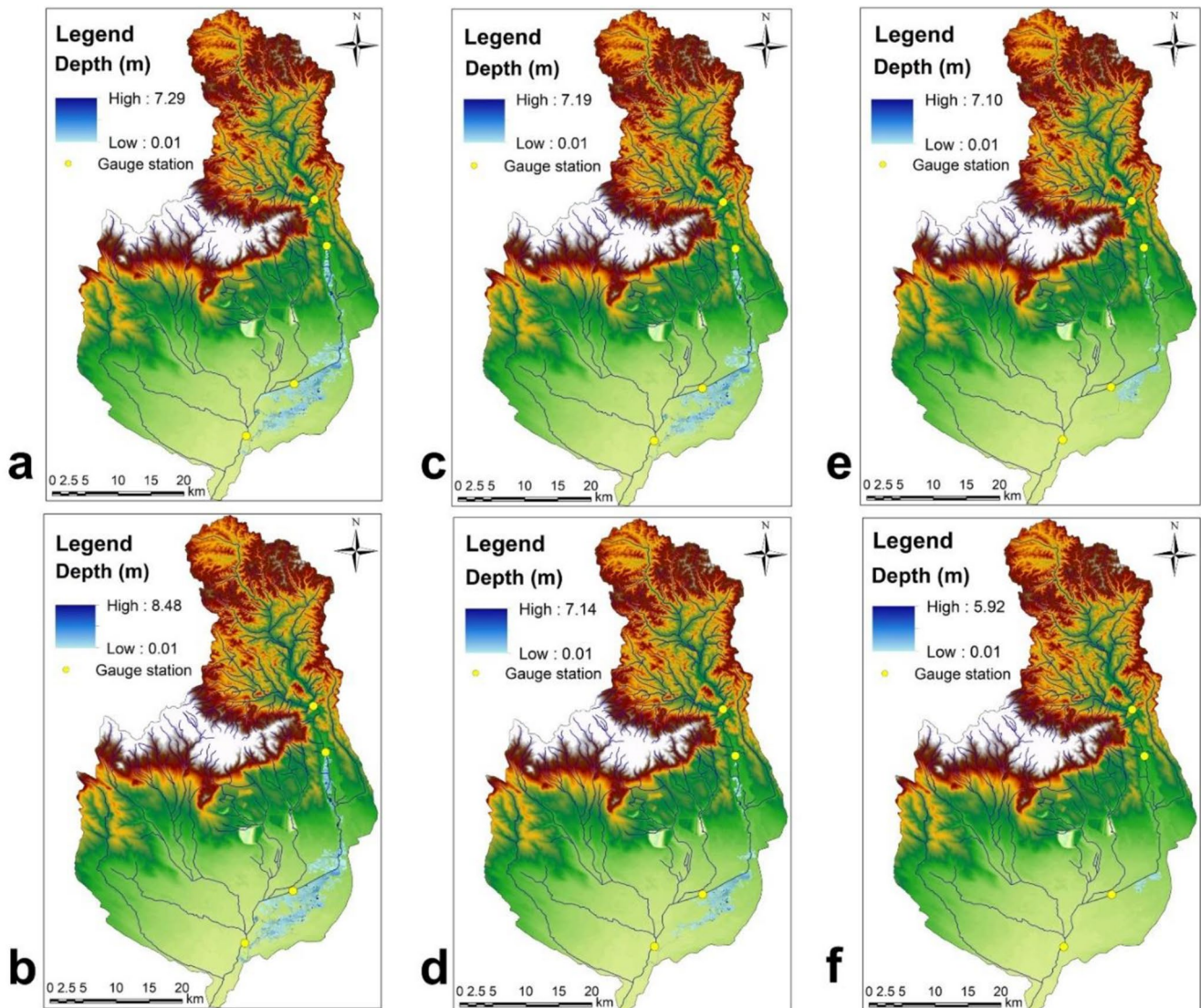


Fig. 2 Spatial representation of the inundation models in the watershed of the Tarna River in northern Hungary: **a, b**=largest flood event, **c, d**=flood event, and **e, f**=average flood event

Table 3 Extent of inundation and values for the three delineated areas (VS: upper section TMS: middle section, TOS: lower section) and total area (C) in the watershed of the Tarna River in northern Hungary. L-a and L-b: largest flood event; F-c and F-d: Flood event; A-e and A-f: average flood event

Event type	Event	VS (km ²)	TMS (km ²)	TOS (km ²)	C (km ²)
Largest	L_a	8.26	37.74	0.88	46.89
	L_b	9.09	39.86	1.41	50.36
Flood	F_c	6.81	33.62	0.47	40.91
	F_d	3.94	18	0.13	22.07
Average	A_e	2.73	8.93	0.02	11.68
	A_f	0.01	2.93	0.01	2.95

relative differences were large. Thus, the NRMSE indicated a large bias. Event F_c yielded identical water levels at the peak points; however, the decrease in water levels was slower than the observed values. F_d also resulted in matching peaks; however, the modeled values were consistently below the observations. The values of event L_a showed a similar trend, with minor variations, where the modeled values were consistently higher. The model of L_b closely

followed the observations, even in the case of high-water levels; however, the decrease was slower in the model. TMS exhibited the most divergent results with respect to water level variations. F_c had a large bias at the peaks, and the model remained consistently below the observed values. Plot F_d did not show a prominent increase in the water levels for the model. Changes in L_a and L_b were tracked in parallel, yet the model results indicated lower water levels. The events in the VS showed similar trends for A_e and A_f. In the case of F_c, the model underperformed the observed values at peaks. The modeled values of the event F_d exhibited an identical trend to the observed values. Regarding event L_a, there was underperformance in the modeled values at the peaks. In the case of L_b, a lower value was observed in the first two prominent peaks of the modeled results (Fig. 3).

Values of event 'b' yielded outstanding results for all areas, as expected, given that this event was characterized by the longest duration and high flow data within the time interval. Subsequently, events 'd', 'a', and 'c' produced similarly good results (Fig. 4). Events 'e' and 'f' exhibited

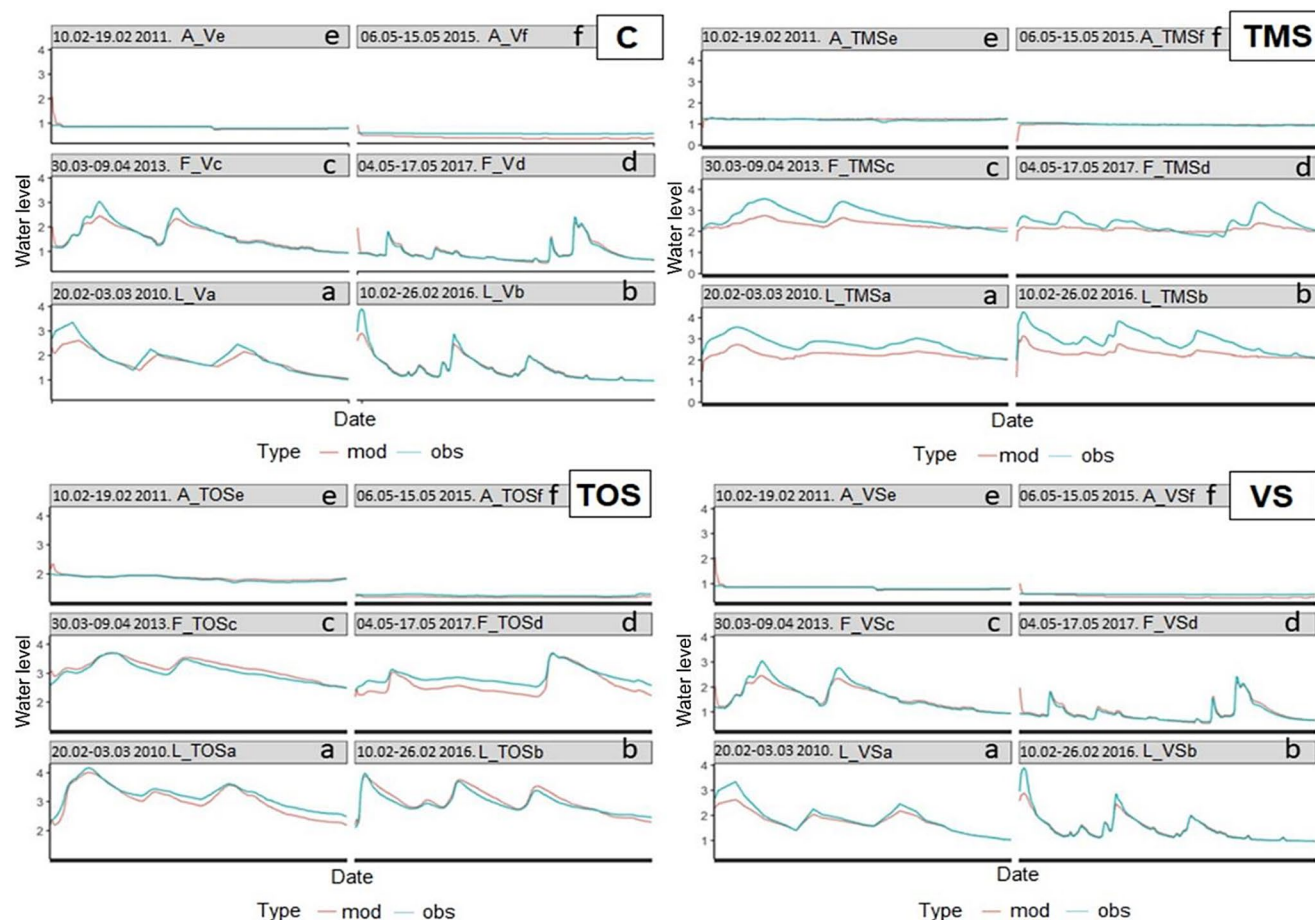


Fig. 3 Spatial and event-based distribution of observed (obs) and modeled (mod) water levels during runs for the watershed of the Tarna River in northern Hungary. C: total area; TMS: middle section; TOS:

lower section; VS: upper section; a, b, c, d, e, and f: largest flood event a, b, flood event c, d, and average flood event e and f, respectively

significant deviations from other events across all areas. As anticipated, these models performed the least favourably, owing to their short time intervals and limited variation in the input data. The average values and accuracy of these events differed from those of the higher and highest water levels.

In the case of the C area, events ‘b’ and ‘c’ yielded results with an RMSE value close to 0.2, while the values for events ‘a’ and ‘d’ fell within the 0.3 range. The values for events ‘e’ and ‘f’ appeared in the Taylor diagram with a large error margin (Fig. 4). An increase in the RMSE indicates a decrease in the model performance. The TMS values showed the largest difference in RMSE in each case. Again, events ‘e’ and ‘f’ performed the poorest. In the application

of the Taylor diagram for water-level assessment, models closer to the centre of the diagram with lower standard deviation values suggest that they are more reliable and can be applied with greater accuracy. Generally, correlation coefficients indicated strong relationships between the modeled and observed values, but there were exceptions, usually in the case of ‘e’ and ‘f’ events where other accuracy metrics also showed low performance. Strong correlations were observed in areas C, TOS, and VS, whereas in TMS, there were two events where the correlation between the models and the measured values ranged between 0 and 0.2 (Fig. 4).

The accuracy of NRMSE ranged from 0 to 1305. Events classified as average consistently produced values that exceeded the average. In the case of A_VSf and A_Cf, the

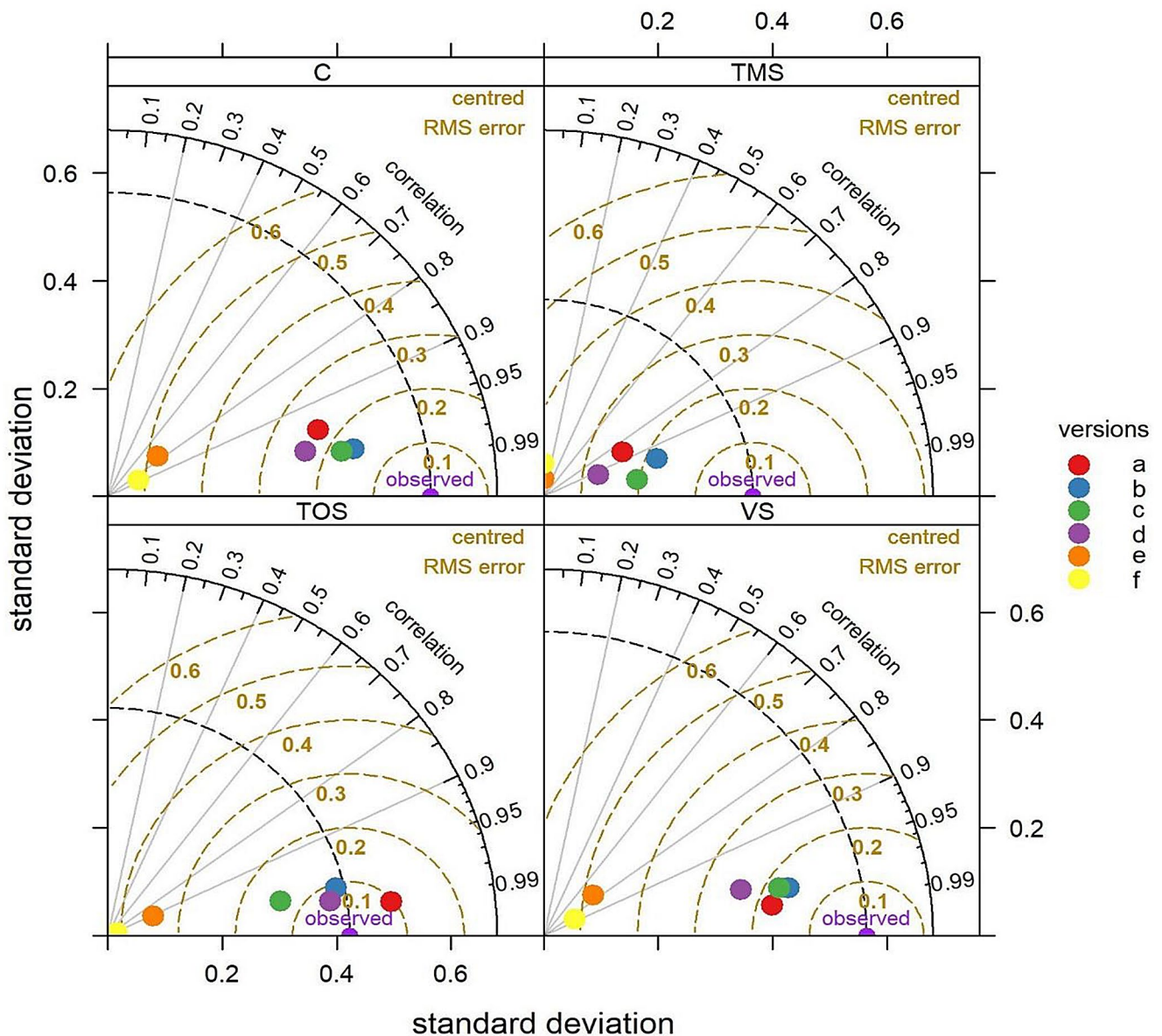


Fig. 4 Taylor diagram of hydrological models by area and event for the watershed of the Tarna River in northern Hungary. C, total area; TMS, middle section; TOS, lower section; VS, upper section. The event codes (versions) correspond to those in Fig. 2

models were less accurate, whereas the models for larger floods generally performed well based on the NRMSE (Fig. 5).

As ubRMSE only reflected the unbiased model error, it did not identify the model performances, but indicated that L_TMSa and L_TMSb, as well as F_TMSc and F_TMSd, had accuracy issues, and we also experienced the same with the NSEs. However, NSE also indicated unsatisfactory results for almost all average (A) models, except for A_TOSe. KGEs usually corresponded to NRMSE and NSE. Based on this metric, the majority of models can be

considered accurate, as 18 out of 24 models performed satisfactorily. Based on the results of the NSE performance metric, in 11 cases, the models performed well in terms of fitting the predicted and observed values, because they were close to the threshold of 1. Generally, the average flow simulations performed the worst, and flood and large flood simulations were more accurate (Fig. 5).

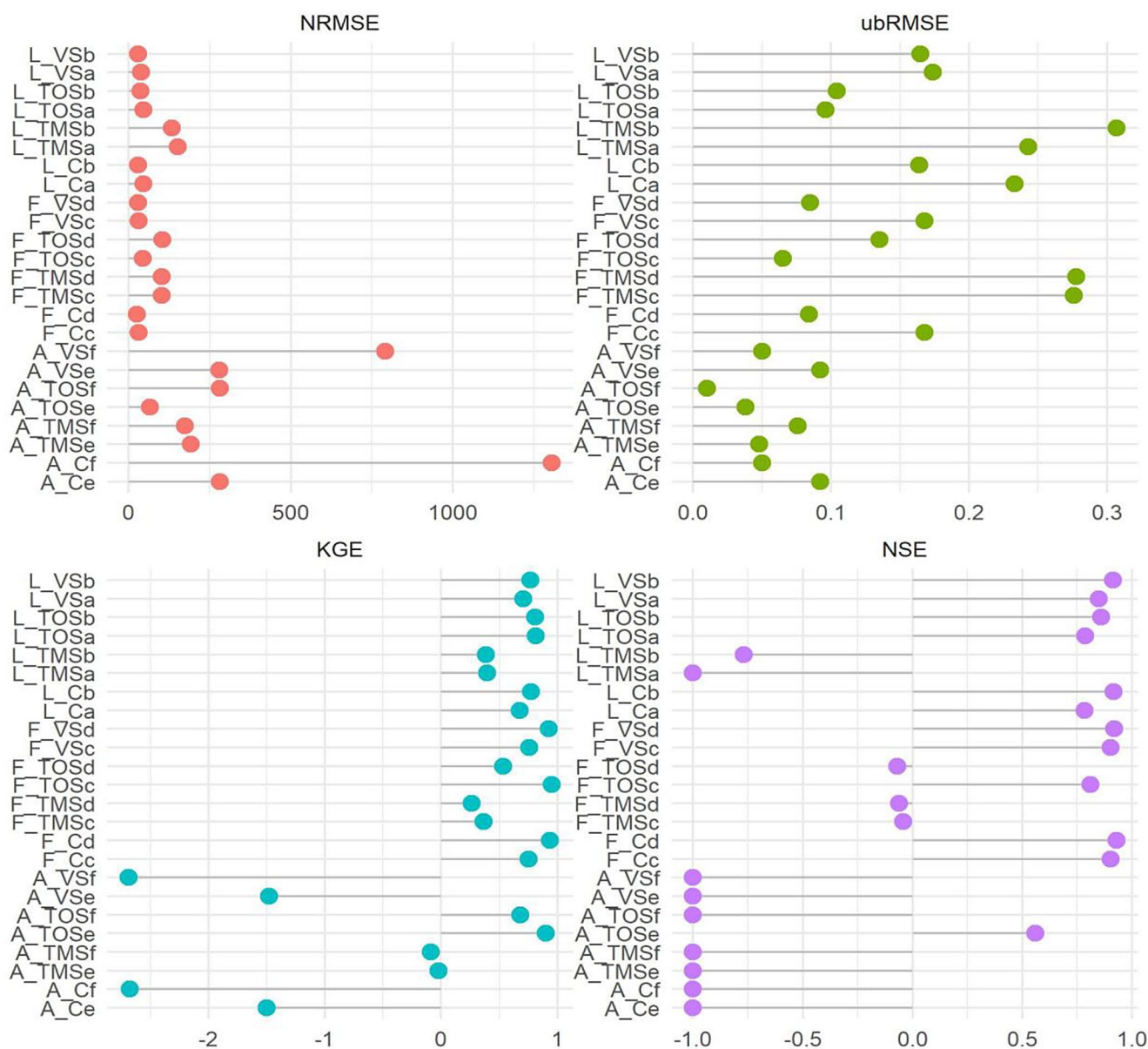


Fig. 5 Accuracy metrics of the model runs for the watershed of the Tarna River in northern Hungary (NRMSE=normalized root mean square error; ubRMSE=unbiased root mean square error; KGE=Kling-Gupta Efficiency; NSE=Nash-Sutcliffe Efficiency). VS,

upper section; TMS, middle section; TOS, lower section; C, total area. L-a and L-b: Largest flood event, F-c and F-d: Flood event, A-e and A-f: Average flood event

4 Discussion

The observed rise in the frequency of flood events after 2005 for the Tarna River has been confirmed. This trend is underscored by the streamflow data spanning from 1990 to 2019. Upper sections had shorter but larger number of floods, but the lowest section, Tarnaõrs (TOS) had both more flood events, and longer flood lengths. These shifts are attributable to trends associated with climate change over recent years [37, 38].

A varying trend in the temporal changes in the measured and modelled water levels was observed. No significant changes were evident during the average events, but during large and major flood events, a discontinuity in the flood wave pattern was observed (Fig. 3). Illés and Konecsny [15] noted that during the 1998 Tisza River flood, discontinuity of the peak flood wave may have occurred because of the gradual filling of the floodplain depressions, i.e., filling the swales, and lower parts of the floodplain behind the natural levees through crevasse channels. Tarna's floodplain has a varying width, thus, the geomorphology also can be a main influencing factor of the changes in the water level during floods: inundations in the floodplain depressions and areas farther from the riverbed influenced the water levels in the riverbed and the peak water levels observed during the recession of the flood wave. Through water level graphs, we demonstrated that the rate of water level change was rapid in VS section events (Fig. 3). In the VS_c and VS_d cases, a steep curve of the values was noted compared with the TMS_c, TMS_d, TOS_c, and TOS_d sections. The VS section represented the upper reach of the Tarna River basin where the steeper slopes of the sub-catchments result in faster flow to lower-lying areas, leading to higher peak values of greater intensity runoff. In the TMS section, characterized by lower, flatter valley floors, the hydrographs increasingly flatten out, indicating prolonged (lasting several days) floods. Similarly, a prolonged flood curve was observed in the TOS section, which was mainly attributable to terrain characteristics. According to Szlávik [39] and Stoffel et al. [40], among the various factors influencing flood wave formation, the effect of topography is one of the most significant, as manifested by the hydrological responses of mountainous and highland areas.

We found that the TMS section had the largest errors in terms of accuracy metrics: according to the accuracy assessment, the TMS section was the weakest, with the highest RMSE values, the ubRMSE and NSE values (Fig. 5) proved to be the least accurate. This result may primarily be explained by the topography data: as SRTM did not include the specific details of the terrain, e.g., the dykes, in reality, floods never inundated the areas outside the dykes. Accordingly, both in spatial and temporal terms the accuracy were

for this section. Furthermore, the water level gauge associated with the TMS section was located in the central part of the delineated area, resulting in larger differences between the modelled and measured data, meaning that water level gauges placed at greater distances provided less accurate model results. The more accurate the measurement results, water level gauges, and data are, the more accurate the model is. According to Tapley et al. [41], observations aid in the linking and understanding of global and regional processes. The interpretation of empirical knowledge and event-based models can help to understand future events and manage risks.

The modeling supported that the terrain data significantly influenced the results and accuracy of the models, as evidenced by inundation maps showing flooding during average events 'e and 'f' (Fig. 2). During events 'a', 'b', 'c', and 'd', it was determined that the TMS section was the most sensitive area, although there were areas in every section where the spatial prediction of inundation or its extent was not accurate, which was also observed in the results of the TMS water levels and the spatial extent of water, as the difference between measured and modelled results was the largest here (Fig. 2). Our results were influenced by the lack of available data and their resolution of the available data. Precise delineation of channel banks was not possible from the available data, and the models indicated inundation in places along the entire section where inundation cannot occur in reality. To achieve better results, a much better digital terrain model is needed, including embankments and road embankments and ditches, beyond the general topographic features. However, this is not unique to small watersheds, but is a common problem with limited availability and usability of data, as pointed out by Brunner et al. [42]. Therefore, compromises must be made regarding the input data and resolution.

However, HEC-RAS modeling provided acceptable results for water level prediction, and the spatial output (predicted inundated areas), at least in the case of floods, proved to be useful. Although the inundations were inaccurate, they showed a potential map if the dykes would breach and road embankments did not impede floods. This result is supported by the findings of Tamiru and Dinka [12], who demonstrated that hydrological models created in the HEC-RAS software environment were suitable for identifying and examining flood inundation areas as part of a flood risk strategy. As expected, the spatial inundation values of the models corresponded with greater inundation occurring in areas with high-water flow and prolonged high-water levels lasting several days. In a study by Ongdas et al. [43], acceptable results were obtained regarding the magnitude of the modelled floods and the extent of the hazard maps. In their study, Moya Quiroga et al. [11] provided evidence

that during flood events, HEC-RAS is suitable for modeling the spread and temporal changes of water. In our investigation, the HEC-RAS models demonstrated good performance; however, we found that the accurate determination of boundary conditions is crucial, as it can result in significant changes in the outcomes during mapping.

Many studies have employed modeling to explore and understand these processes. Chen et al. [44] investigated the relationship between river flow and floodplain areas. Zhang et al. [45] summarized the diversity of hydrological models and the importance of environmental parameters in various aspects. Previous studies have addressed small watershed modeling in different software environments, such as MIKE-SHE [46–48]. Czigány et al. [49] also conducted flood modeling on smaller areas of Hungary; however, they used the HEC-HMS software environment [49]. In Hungary, previous modeling efforts have been undertaken; however, they employed different methodologies and pursued distinct objectives.

Although the modeling process can vary significantly in several aspects, comparing the results aids in enhancing the process and accuracy of hydrological modeling. In their research, Chen et al. [44] also concluded that the river hydrodynamic model effectively reproduces the hydrological conditions. Moreover, they found that large floods lead to shorter residence times and flow path lengths in floodplains, but result in increased cross-boundary flow within the river section. Tamiru and Dinka [12] found that the HEC-RAS model results and NDWI values were consistent 94.6% and 96% of the time during the calibration and validation periods, respectively, aiding in the improvement of flood forecasting models. Similarly, in their hydrological modeling research, Ogras and Onen [23] emphasized the importance of current topographical and hydrological data for the area, suggesting that the modeling results can predict potential scenarios over several decades. Our current research, similar to the findings of the aforementioned researchers, also yielded promising results.

For further investigation, it is essential to consider a significant error factor: during an event, the streamflow of the tributaries can greatly influence the flow of the Tarna River. The study was relevantly limited by data scarcity, availability of accessible high-resolution digital elevation models, lack of gauges, and the distances were large between existing gauges. The most significant challenge in parameterizing the models was the accurate determination of the riverbanks. As a future research opportunity, detailed geodetic surveying of the riverbank, precise determination of the shoreline zone, and parameterization of tributaries flowing into the Tarna River, including determination of their flow rates. With this data, we would have the opportunity for complex hydrological model construction, which would

provide answers to further emerging questions compared to the current research. The data obtained from drone-based photogrammetric surveys can serve as a suitable starting point and reference point for evaluating the data generated during this research.

5 Conclusions

Our goal was to assess the possibilities and accuracy of hydrological modeling considering topographic characteristics, using event-based time series as input data in a data-deficient environment. Our findings of the inundation mapping showed that in the area we defined as the middle section, the extent of inundation was the largest. This was followed by the upper section, which had the highest topographic elevation values. The smallest inundation was observed in the lower section. However, to increase accuracy, we recommend using more detailed topographic data as a base, thus avoiding the inaccurate determination of boundary conditions and riverbank edges. Similar trends were observed in the modelled and observed water levels throughout all sections. Thus, segmenting smaller areas may not consistently offer resolution in all instances. Based on the results of the model divided into three areas, we recommend interpreting water levels and spatial inundations together in future event-based modeling to create a comprehensive understanding. The accuracy assessment indicated that the values for the event “Largest Flood” produced excellent results across all areas, followed closely by the events “Flood” which also yielded similarly positive outcomes. Our hypothesis was confirmed in case of flood event of the longest duration and highest water levels. The NRMSE accuracy metrics confirmed that the models for larger flood events generally performed well. “Average” events typically performed poorly according to the accuracy metrics. Although the results showed discrepancies in event-based modeling, in data-limited environments, such models can still aid in mitigating the spread of water during potential flood events and facilitate more effective decision-making processes for stakeholders.

Acknowledgements This research was conducted within the framework of the Doctoral School of Earth Sciences at the University of Debrecen. The research was supported by the RRF-2.3.1-21-2022-00008 project.

Funding Open access funding provided by University of Debrecen.

Declarations

Conflict of interest The authors declare that they have not have any known financial interests or personal relationships that may have influenced the work described in this paper.

Open Access This article is licensed under a Creative Commons Attribution 4.0 International License, which permits use, sharing, adaptation, distribution and reproduction in any medium or format, as long as you give appropriate credit to the original author(s) and the source, provide a link to the Creative Commons licence, and indicate if changes were made. The images or other third party material in this article are included in the article's Creative Commons licence, unless indicated otherwise in a credit line to the material. If material is not included in the article's Creative Commons licence and your intended use is not permitted by statutory regulation or exceeds the permitted use, you will need to obtain permission directly from the copyright holder. To view a copy of this licence, visit <http://creativecommons.org/licenses/by/4.0/>.

References

- Trenberth, P., Ambenje, J., Bojariu, R., Easterling, D., Tank, K., Parker, D. (2007). Observations: Surface and Atmospheric Climate Change. 235–336.
- Pal, J. S., Giorgi, F., & Bi, X. (2004). Consistency of recent European summer precipitation trends and extremes with future regional climate projections. *Geophysical Research Letters*, 31(13), L13202–L13201. <https://doi.org/10.1029/2004GL019836>
- Christensen, J., & Christensen, O. (2003). Severe summer-time flooding in Europe. *Nature*, 421, 805–806. <https://doi.org/10.1038/421805a>
- Bartholy, J., Pongrácz, R., & Kis, A. (2015). Projected changes of extreme precipitation using multi-model approach. *Időjárás*, 119, 129–142.
- Alfieri, L., Cohen, S., Galantowicz, J., Schumann, G. J., Trigg, M. A., Zsoter, E., Prudhomme, C., et al. (2018). Global network for operational flood risk reduction. *Environmental Science & Policy*, 84, 149–158. <https://doi.org/10.1016/j.envsci.2018.03.014>
- Eilander, D., Couasnon, A., Leijnse, T., Ikeuchi, H., Yamazaki, D., Muis, S., & Ward, P. J. (2023). A globally applicable framework for compound flood hazard modeling. *Natural Hazards and Earth System Sciences*, 23(2), 823–846. <https://doi.org/10.5194/nhess-23-823-2023>
- Szlávik, L. (2003). Az ezredforduló árvizeinek és belvizeinek hidrológiai jellemzése. *Vízügyi Közlemények*, 85(4), 547–570.
- Pirkhoffer, E., Czigány, S., Hegedűs, P., Balatonyi, L., & Lóczy, D. (2013). Lefolyási viszonyok talajszempontú analízise ultrakisméretű vízgyűjtőkön [Soil-based analysis of runoff conditions in ultra-small watersheds]. *Tájéközlelőlapok | Journal of Landscape Ecology*, 11(1), 105–123. <https://doi.org/10.56617/tl.3737>
- Lóczy, D., Czigány, S., & Pirkhoffer, E. (2012). Flash flood hazards. In M. Kumarasamy (Eds.), *Studies on Water Management Issues*. (pp. 27–52). IntechOpen. <https://doi.org/10.5772/28775>
- Dottori, F., Salamon, P., Bianchi, A., Alfieri, L., Hirpa, F. A., & Feyen, L. (2016). Development and evaluation of a framework for global flood hazard mapping. *Advances in Water Resources*, 94, 87–102. <https://doi.org/10.1016/j.advwatres.2016.05.002>
- Moya Quiroga, V. M., Kurea, S., Udoa, K., & Manoa, A. (2016). Application of 2D numerical simulation for the analysis of the February 2014 Bolivian Amazonian flood: Application of the new HEC-RAS version 5. *Ribagua*, 3(1), 25–33. <https://doi.org/10.1016/j.riba.2015.12.001>
- Tamiru, H., & Wagari, M. (2022). Machine-learning and HEC-RAS integrated models for flood inundation mapping in Baro River Basin, Ethiopia. *Modeling Earth Systems and Environment*, 8(2), 2291–2303. <https://doi.org/10.1007/s40808-021-01175-8>
- García-Alén, G., González-Cao, J., Fernández-Nóvoa, D., Gómez-Gesteira, M., Cea, L., & Puertas, J. (2022). Analysis of two sources of variability of basin outflow hydrographs computed with the 2D shallow water model Iber: Digital Terrain Model and unstructured mesh size. *Journal of Hydrology*, 612, 128182. <https://doi.org/10.1016/j.jhydrol.2022.128182>
- Kenward, T., Lettenmaier, D. P., Wood, E. F., & Fielding, E. (2000). Effects of digital elevation model accuracy on hydrologic predictions. *Remote Sensing of Environment*, 74(3), 432–444. [https://doi.org/10.1016/S0034-4257\(00\)00136-X](https://doi.org/10.1016/S0034-4257(00)00136-X)
- Illés, L., & Konecsny, K. (2003). Az 1998. november árhullám hidrológiai értékelése a Tisza-völgyi árvizek sorában [Hydrological assessment of the November 1998 flood wave in the series of floods in the Tisza Valley]. *Vízügyi Közlemények, Special Issue 2003(1)*, Az 1998. évi árvíz [The flood of 1998.], 77–84.
- Sziebert, J., & Zellei, L. (2003). Árvízi áramlásmérések tapasztalatai a Tiszán [Experiences from flood flow measurements on the Tisza River.]. *Vízügyi Közlemények, Special issue 2003(1)*, Elemző és módszertani tanulmányok Az 1998–2001. évi ár- és belvizekről [Analytical and methodological studies on floods and inland waters from 1998 to 2001.], 133–144.
- Bernhofen, M. V., Cooper, S., Trigg, M., Mdee, A., Carr, A., Bhave, A., Solano-Correa, Y. T., et al. (2022). The role of global data sets for riverine flood risk management at national scales. *Water Resources Research*, 58(4), e2021WR031555. <https://doi.org/10.1029/2021WR031555>
- Wang, X., & Xie, H. (2018). A review on applications of remote sensing and geographic information systems (GIS) in water resources and flood risk management. *Water*, 10(5), 608. <https://doi.org/10.3390/w10050608>
- Zeiger, S. J., & Hubbard, J. A. (2021). Measuring and modeling event-based environmental flows: An assessment of HEC-RAS 2D rain-on-grid simulations. *Journal of Environmental Management*, 285, 112125. <https://doi.org/10.1016/j.jenvman.2021.112125>
- Pregun, C., Tamás, J., Takács, P., & Bíró, T. (2006). HEC-RAS alapú geodatabázis vizsgálata az EU Vízügyi Keretirányelv előírásai alapján I. [Examination of HEC-RAS-based geodatabase in accordance with the requirements of the EU Water Framework Directive I]. *Acta Agraria Kaposváriensis*, 10(1), 31–42.
- Pirkhoffer, E., Czigány, S., Geresdi, I., & Nagyvárad, L. (2009). Impact of rainfall pattern on the occurrence of flash floods in Hungary. *Zeitschrift für Geomorphologie Supplement*, 53(2), 139–157. <https://doi.org/10.1127/0372-8854/2009/0053S3-0139>
- Murányi, G., & Koncsos, L. (2022). Examination of a nature-based flood control solution in the Tisza River Valley nearby Csongrád town with HEC-RAS 1D-2D coupled model (in Hungarian). *Hungarian Journal of Hydrology*, 102(1), 13–24.
- Ogras, S., & Onen, F. (2020). Flood analysis with HEC-RAS: A case study of Tigris River. *Advances in Civil Engineering*, 2020, 1–13. <https://doi.org/10.1155/2020/6131982>
- Costabile, P., Costanzo, C., Ferraro, D., Macchione, F., & Petaccia, G. (2020). Performances of the new HEC-RAS version 5 for 2-d hydrodynamic-based rainfall-runoff simulations at basin scale: Comparison with a state-of-the-art model. *Water*, 12, 2326. <https://doi.org/10.3390/w12092326>
- Tamiru, H., & Dinka, M. O. (2021). Application of ANN and HEC-RAS model for flood inundation mapping in lower Baro Akobo River Basin, Ethiopia. *Journal of Hydrology: Regional Studies*, 36, 100855. <https://doi.org/10.1016/j.ejrh.2021.100855>
- Szlávik, L. (2003). A 2001. évi felső-tiszai árvíz kialakulása és hidrológiai sajátosságai. *Vízügyi Közlemények*, 85(4), 13–34.
- Szigyártó, Z. (2015). A Tisza nagyvízi vízjárása a múlt század elejétől napjainkig. *Hidrológiai Közöny*, 95(4), 19–29.
- Kovács, S., Lovas, A., & Gombás, K. (2015). Flood protection of Hungary in the integrated water management in the Tisza River Valley as an example. *Hidrológiai Közöny*, 95(4), 6–19.
- Nagy, I. (2013). Javaslatok a magyar árvízvédelem megújításához. *Hidrológiai Közöny*, 93(1), 15–23.

30. Gashi, N., Czigány, S., Pirkhoffer, E., & Kiss, K. (2023). Modeling the impact of climate change on the flow regime and channel planform evolution of the lower Drava River. *Modern Geográfia*, 18(2), 47–76. <https://doi.org/10.15170/MG.2023.18.02.04>
31. Gábris, G. (2011). A zagyva–tarna alföldi vízrendszerének kialakulása és fejlődése [The formation and development of the Zagyva-Tarna lowland water system]. *Földrajzi Közlemények*, 135(3), 205–218.
32. Tanács, E., Belényesi, M., Lehoczki, R., Pataki, R., Petrik, O., Standovár, T., & Maucha, G. (2022). Compiling a high-resolution country-level ecosystem map to support environmental policy: Methodological challenges and solutions from Hungary. *Geocarto International*, 37(25), 8746–8769. <https://doi.org/10.1080/10106049.2021.2005158>
33. QGIS DEVELOPMENT TEAM (2019). QGIS Geographic Information System. Open Source Geospatial Foundation Project. <http://qgis.osgeo.org>
34. US Army Corps of Engineers (USACE). (2016). *HEC-RAS river analysis system. Hydraulic reference manual*. Hydrologic Engineering Research Center.
35. Zeybek, M. (2018). Nash-Sutcliffe efficiency approach for quality improvement. *Journal of Applied Mathematics and Computation*, 2(11), 496–503. <https://doi.org/10.26855/jamc.2018.11.001>
36. R Core Team (2018). R: A language and environment for statistical computing. Vienna, Austria: R Foundation for Statistical Computing. Retrieved from <https://cran.r-project.org/>
37. Ilyés, C., Szűcs, P., & Turai, E. (2022). Appearance of climatic cycles and oscillations in Carpathian Basin precipitation data. *Hungarian Geographical Bulletin*, 71(1), 21–37. <https://doi.org/10.15201/hungeobull.71.1.2>
38. Kis, A., Szabó, P., & Pongrácz, R. (2023). Spatial and temporal analysis of drought-related climate indices for Hungary for 1971–2100. *Hungarian Geographical Bulletin*, 72, 223–238. <https://doi.org/10.15201/hungeobull.72.3.2>
39. Szlávik, L. (2021). The March 2001 flood disaster in Bereg was 20 years ago. *Hungarian Journal of Hydrology*, 101(2), 3–25.
40. Stoffel, M., Wyżga, B., & Marston, R. A. (2016). Floods in mountain environments: A synthesis. *Geomorphology*, 272, 1–9. <https://doi.org/10.1016/j.geomorph.2016.07.008>
41. Tapley, B. D., Bettadpur, S., Ries, J. C., Thompson, P. F., & Watkins, M. M. (2004). GRACE measurements of mass variability in the Earth system. *Science*, 305(5683), 503–505. <https://doi.org/10.1126/science.1099192>
42. Brunner, M. I., Slater, L., Tallaksen, L. M., & Clark, M. (2021). Challenges in modeling and predicting floods and droughts: A review. *Wiley Interdisciplinary Reviews: Water*, 8(3), e1520. <https://doi.org/10.1002/wat2.1520>
43. Ongdas, N., Akiyanova, F., Karakulov, Y., Muratbayeva, A., & Zinabdin, N. (2020). Application of HEC-RAS (2D) for flood hazard maps generation for Yesil (Ishim) river in Kazakhstan. *Water*, 12(10), 2672. <https://doi.org/10.3390/w12102672>
44. Chen, X., Chen, L., Stone, M. C., & Acharya, K. (2020). Assessing connectivity between the river channel and floodplains during high flows using hydrodynamic modeling and particle tracking analysis. *Journal Hydrology*, 583, 124609. <https://doi.org/10.1016/j.jhydrol.2020.124609>
45. Zhang, Y., Huang, C., Zhang, W., Chen, J., & Wang, L. (2021). The concept, approach, and future research of hydrological connectivity and its assessment at multiscales. *Environmental Science and Pollution Research*, 28(38), 52724–52743. <https://doi.org/10.1007/s11356-021-16148>
46. Aredo, M. R., Hatiye, S. D., & Pingale, S. M. (2021). Impact of land use/land cover change on stream flow in the Shaya catchment of Ethiopia using the MIKE SHE model. *Arabian Journal of Geosciences*, 14, 114. <https://doi.org/10.1007/s12517-021-06447-2>
47. Paudel, S., & Benjankar, R. (2022). Integrated hydrological modeling to analyze the effects of precipitation on surface water and groundwater hydrologic processes in a small watershed. *Hydrology*, 9(2), 37. <https://doi.org/10.3390/hydrology9020037>
48. Singh, R., Subramanian, K., & Refsgaard, J. C. (1999). Hydrological modelling of a small watershed using MIKE SHE for irrigation planning. *Agricultural Water Management*, 41(3), 149–166. [https://doi.org/10.1016/S0378-3774\(99\)00022-0](https://doi.org/10.1016/S0378-3774(99)00022-0)
49. Czigány, S., Pirkhoffer, E., Lóczy, D., & Balatonyi, L. (2013). Flash flood analysis for Southwest-Hungary. In Lóczy, D. (Eds.): *Geomorphological Impacts of Extreme Weather: Case Studies from Central and Eastern Europe*. (pp. 67–82) Dordrecht: Springer Science and Business Media. https://doi.org/10.1007/978-94-007-6301-2_5

Publisher's note Springer Nature remains neutral with regard to jurisdictional claims in published maps and institutional affiliations.